



Thermally activated martensite formation in ferrous alloys

Villa, Matteo; Somers, Marcel A. J.

Published in:
Scripta Materialia

Link to article, DOI:
[10.1016/j.scriptamat.2017.08.024](https://doi.org/10.1016/j.scriptamat.2017.08.024)

Publication date:
2017

Document Version
Peer reviewed version

[Link back to DTU Orbit](#)

Citation (APA):
Villa, M., & Somers, M. A. J. (2017). Thermally activated martensite formation in ferrous alloys. *Scripta Materialia*, 142, 46-49. <https://doi.org/10.1016/j.scriptamat.2017.08.024>

General rights

Copyright and moral rights for the publications made accessible in the public portal are retained by the authors and/or other copyright owners and it is a condition of accessing publications that users recognise and abide by the legal requirements associated with these rights.

- Users may download and print one copy of any publication from the public portal for the purpose of private study or research.
- You may not further distribute the material or use it for any profit-making activity or commercial gain
- You may freely distribute the URL identifying the publication in the public portal

If you believe that this document breaches copyright please contact us providing details, and we will remove access to the work immediately and investigate your claim.

Thermally activated martensite formation in ferrous alloys

Matteo Villa*, Marcel A.J. Somers

Technical University of Denmark, Department of Mechanical Engineering,

Produktionstorvet, Building 425, DK 2800 Kgs. Lyngby, DK

matv@mek.dtu.dk, somers@mek.dtu.dk

Abstract

Magnetometry was applied to investigate the formation of α/α' martensite in 13 ferrous alloys during immersion in boiling nitrogen and during re-heating to room temperature at controlled heating rates in the range 0.0083-0.83 K s⁻¹. Data shows that in 3 of the alloys, those that form {5 5 7}_γ martensite, no martensite develops during cooling. For all investigated alloys, irrespective of the type of martensite forming, thermally activated martensite develops during *heating*. The activation energy for thermally activated martensite formation is in the range 8–27 kJ mol⁻¹ and increases with the fraction of interstitial solutes in the alloy.

Key words: martensitic phase transformations; steel; kinetics

Evidence of thermally activated, i.e. time dependent, martensite formation was firstly reported by Kurdjumov and Maximova [1] who showed an increase in magnetization during isothermal holding of Fe-based alloys at cryogenic temperatures as well as during continuous heating from 77 K.

The authors interpreted the kinetics of transformation in terms of time-dependent

* corresponding author; Tel: +45 45252221; Fax: 45251961

1 nucleation and growth of martensite and obtained an activation energy for time-
2
3 dependent martensite formation, E_A , equal to 7 kJ mol^{-1} by applying an Arrhenius type
4
5 analysis. E_A was conceived as the sum of two terms (see Ref. [2]): a temperature-
6
7 dependent activation energy for nucleation and a constant activation energy for growth.
8
9

10 Thermally-activated growth of martensite implies that at a sufficiently low
11
12 temperature, say lower than 77 K , the transformation cannot progress at an
13
14 experimentally observable rate, i.e. infinitely slow. Kulin and Cohen showed as early as
15
16 1950 that this is not the case, and martensite formation can easily occur at a temperature
17
18 as low as the boiling point of Helium [3], 4 K . Additionally, Bunshah and Mehl [4]
19
20 firstly demonstrated in 1953 that at 77 K the formation of several units of martensite can
21
22 take place within $1 \mu\text{s}$ and that the growth rate of the units can be independent of
23
24 temperature within a significantly large temperature interval (i.e. growth is athermal).
25
26
27
28
29

30 Based on these early observations, Cohen and co-workers developed a nucleation-
31
32 controlled description of the kinetics of martensite formation, where nucleation of
33
34 martensite is time dependent and growth is instantaneous. Moreover, beyond a certain
35
36 threshold value of the driving force for transformation, ΔG^* , nucleation of martensite is
37
38 considered not suppressible [5].
39
40
41

42 In the following 60 years, Cohen's approach has been declined in different forms (see
43
44 Refs. [6,7]). The transformation has been studied at the onset of the process and E_A has
45
46 been evaluated from the time necessary to reach a fixed (small) fraction of martensite,
47
48 say 0.2% , in a series of isothermal tests conducted for $\Delta G < \Delta G^*$ (where ΔG is the
49
50 driving force for transformation). According to this approach, E_A is proportional to the
51
52 energy barrier for nucleation of the most potent nuclei in the material and is a linear
53
54 function of ΔG .
55
56
57
58
59
60
61
62
63
64
65

1 In the form presented by Kakeshita et al. [8], the nucleation-controlled approach can
2 accurately describe the start of isothermal transformation in several ferrous and non-
3 ferrous systems. Moreover, the theory remains consistent whether ΔG is varied by
4 varying the temperature, by applying a magnetic field or by applying a hydrostatic
5 pressure. Nevertheless, a series of experimental observations remains not addressed by
6 the current theories.
7

8 Firstly, slow growth of martensite was demonstrated as early as 1953 [9]. Slow
9 growth of martensite has historically been interpreted as an exception caused by
10 relaxation processes at a free surface, and was henceforth neglected.
11

12 Secondly, it has been established that in ferrous alloys the formation of martensite at
13 high temperatures can be suppressed by fast cooling [10-12]. This observation cannot be
14 reconciled with insuppressible nucleation of martensite at the martensite start
15 temperature, M_s , where $\Delta G = \Delta G^*$, followed by instantaneous growth of the martensite
16 units.
17

18 Lastly, it has been established that the critical cooling rate for suppressing martensite
19 formation in Fe depends logarithmically on the fraction of C atoms in the alloy [12].
20 Sofar, this observation has remained unexplained.
21

22 Evidently, a new approach is necessary to reconcile all experimental data. This
23 approach should account for the validity of nucleation-controlled descriptions in a large
24 number of cases, for the possibility of instantaneous formation of martensite at 4 K, for
25 the possibility of slow growth of martensite, and finally for the effect of C content on
26 the critical cooling rate for suppressing martensite formation at high temperature.
27

28 In the present work, isochronal analysis was applied to altogether 13 ferrous alloys
29
30
31
32
33
34
35
36
37
38
39
40
41
42
43
44
45
46
47
48
49
50
51
52
53
54
55
56
57
58
59
60
61
62
63
64
65

(Table 1), including a re-evaluation of those from previous work [14]. The formation of martensite was monitored applying magnetometry, implying that only ferromagnetic α/α' martensite is revealed; paramagnetic ε martensite, if any, remains unobserved. Details on material preparation, experimental setup and quantitative phase analysis were reported earlier [13-15].

Table 1. Sample geometries, austenitization treatment and alloying (in wt-%) of the 13 ferrous alloys. Sample geometry is expressed as either diameter of disks \varnothing or diagonal of square plates D (in mm) / thickness (in mm). Austenitization conditions are expressed as temperature (in K) / time (in ks).

Alloy	Geometry	Austenitization	N	C	Cr	Ni	Mn	Si	Mo	Cu	Ti	Al
2.2N	D 3 / 0.025	923 / 1.8	2.2	-	-	-	-	-	-	-	-	-
1.8N	D 3 / 0.025	923 / 1.8	1.8	-	-	-	-	-	-	-	-	-
1.6C	\varnothing 3 / 0.7	1353 / 0.18	-	1.59	-	-	-	-	-	-	-	-
1.2C	\varnothing 3 / 0.7	1353 / 0.18	-	1.20	-	-	-	-	-	-	-	-
1C	\varnothing 3 / 0.7	1353 / 0.18	-	0.97	-	-	-	-	-	-	-	-
100Cr6	\varnothing 3 / 0.7	1353 / 0.18	-	0.96	1.6	0.1	0.1	0.3	-	0.2	-	-
12Cr-0.7C	\varnothing 2.2 / 0.7	1453 / 0.3	-	0.67	11.5	-	1.0	0.6	-	0.2	-	-
17Cr-0.4C	\varnothing 3 / 0.7	1453 / 0.3	-	0.38	17.0	2.1	0.5	0.5	0.1	0.4	-	0.2
17Cr-0.2C	\varnothing 3 / 0.7	1453 / 0.3	-	0.19	17.0	2.1	0.5	0.5	0.1	0.4	-	0.2
15-7PH	D 3 / 0.25	1253 / 0.3	-	0.09	15.5	7.1	0.6	0.8	2.1	0.4	-	1.2
17-7PH	D 3 / 0.15	1253 / 0.3	-	0.08	17.0	7.0	0.5	0.6	-	0.3	-	1.1
12Cr-9Ni	D 3 / 0.7	1453 / 0.3	-	0.02	12.0	8.6	0.3	0.4	3.5	1.9	0.9	0.4
15Cr-13Ni	\varnothing 3 / 1	1323 / 1.8	-	<0.001	15.3	12.7	-	-	-	-	-	-

The investigations consisted of two types of tests: *ex situ* tests and *in situ* tests. The *ex situ* tests consisted of measuring the magnetization of the samples prior to sub-zero Celsius treatment and after additional immersion in boiling nitrogen and (up-quenching) in water. In the *in situ* tests, the magnetization of the samples was measured straight after immersion in boiling nitrogen, at approx. 80 K, and thereafter monitored during isochronal heating to 280 K. With the exception of 15Cr-13Ni, the applied heating rates were in the range 0.0083-0.167 K s⁻¹. The 15Cr-13Ni alloy was heated at rates in the

range 0.05-0.83 K s⁻¹ to elucidate the initial acceleration of the transformation on continuous heating (see below). Results are presented in Table 2 and Fig. 1.

Table 2. Molar fraction of α/α' martensite f versus thermal step: RT refers to the material after cooling to room temperature; BN after additional immersion in boiling nitrogen; BN-W after additional immersion in boiling nitrogen and re-heating in water; BN-RH after additional immersion in boiling nitrogen and controlled re-heating at the slowest applied rate. Δf_{MAX} is the additional fraction of martensite formed during heating measured at the maximum of the transformation rate. For 15-7PH, metallography indicated the presence of approx. 10% δ -Fe, which is included in the calculation of f .

Alloy	Group	Type of martensite	f_{RT}	f_{BN}	f_{BN-W}	f_{BN-RH}	Δf_{MAX}
2.2N	I	{2 5 9} γ	1%	35%	38%	52%	8.5%
1.8N	I	{2 5 9} γ	32%	53%	62%	77%	8.0%
1.6C	I	{2 2 5} γ + {2 5 9} γ	57%	85%	86%	90%	1.4%
1.2C	I	{2 2 5} γ	81%	94%	94%	97%	1.0%
1C	I	{2 2 5} γ	89%	94%	95%	98%	1.5%
100Cr6	I	{2 2 5} γ + {2 5 9} γ	59%	79%	80%	86%	1.6%
12Cr-0.7C	I	{2 2 5} γ	5%	64%	66%	77%	3.3%
17Cr-0.4C	I	{2 5 9} γ	1%	34%	37%	63%	6.7%
17Cr-0.2C	I	{5 5 7} γ + {2 5 9} γ	16%	55%	64%	78%	5.9%
15-7PH	II	{5 5 7} γ	13%	13%	15%	99%	-
17-7PH	II	{5 5 7} γ	7%	7%	12%	93%	-
12Cr-9Ni	II	{5 5 7} γ	79%	79%	79%	91%	-
15Cr-13Ni	I	{1 1 2} γ	-	21%	21%	27%	1.1%

Table 2 shows that all the alloys under investigation, except for 15Cr-13Ni, are partly martensitic after cooling to room temperature (column f_{RT}). Additional formation of martensite can be promoted at sub-zero Celsius temperatures. From a kinetics point of view, alloys can be classified into two groups, labelled I and II, respectively. For all alloys of group I, immersion in boiling nitrogen promotes instantaneous formation of martensite (compare columns f_{RT} and f_{BN}); for the alloys of group II no (additional)

1 martensite forms during cooling.
2

3 Strikingly, in all investigated alloys and steels martensite formation is observed
4 during (re-)heating (compare columns f_{BN} and f_{BN-W} , f_{NBN-RH}) irrespective of whether no
5 or abundant martensite had formed during cooling to 77 K. The amount of martensite
6 formed during heating is consistently highest for the slowest heating rate (compare
7 columns f_{BN-W} and f_{NBN-RH}).
8
9

10 Fig. 1 shows that, with the exception of 15Cr-13Ni, the transformation on heating
11 starts slowly, accelerates with increasing temperature, and finally slows down before
12 reaching 280 K. In 15Cr-13Ni the transformation shows two distinct accelerations,
13 maybe in connection with the occurrence of two overlapping transformation processes
14 like, for example, the conversion of ϵ martensite into α and the direct formation of α
15 martensite from austenite.
16
17
18
19
20
21
22
23
24
25
26
27
28
29

30 Consistent for all alloys investigated, the transformation curves are shifted towards
31 higher temperatures on faster heating. This is clear evidence that martensite formation
32 during heating is thermally activated.
33
34
35
36

37 The activation energy E_A of the thermally activated mechanism that governs the rate
38 of the transformation can be determined with a Kissinger-like analysis, where $\ln(T_{f'}^2/\phi)$
39 depends linearly on $1/T_{f'}$ and the slope equals E_A/R . Here, $T_{f'}$ is the temperature
40 corresponding to a fixed stage of transformation, f' , and ϕ is the heating rate (cf. Ref.
41 [16]); f' is interpreted as the fraction of martensite developed during re-heating Δf .
42
43
44
45
46
47
48
49

50 E_A was evaluated every increment in Δf by 0.001 for the range $0.005 \leq \Delta f \leq$
51 Δf_{MAX} , where Δf_{MAX} applies at the maximum transformation rate. For each of the alloys
52 of group I, the maximum transformation rate occurred at a fixed transformed fraction,
53 while for the alloys of group II, Δf_{MAX} is a function of the heating rate. In this case, the
54
55
56
57
58
59
60
61
62
63
64
65

1 minimum value of Δf_{MAX} , which is reported for the fastest applied heating of 0.167 K s^{-1} ,
2
3 was used. The interval for Δf was chosen to secure sufficient experimental accuracy
4
5 and to ensure that the analysis is applied sufficiently far from equilibrium [17]. The
6
7 following additional criteria for validity were taken: the linear regression coefficient
8
9 obtained for the linear dependence of $\ln(T_f^{-2}/\phi)$ on $1/T_f$ should be better than 0.9; the
10
11 isochronal cycle should have ran for at least 60 s. These criteria ensure that a linear fit
12
13 of data is realistic and that the heating rate experienced by the sample corresponds to the
14
15 set heating rate, respectively. Our earlier results presented in Ref. [14] were re-evaluated
16
17 according to these criteria.
18
19
20
21
22

23 All evaluated activation energies meeting the above criteria are collected in Fig. 2
24
25 versus the atomic fraction of interstitials. The data is presented such that the error bars
26
27 in E_A are given as the minimum, maximum and average values taking into account the
28
29 standard error of the estimate for linear regression. With the exception of the Fe-N
30
31 alloys, the N-content was assumed negligible.
32
33
34

35 Fig. 2 shows that E_A ranges from 8 to 27 kJ mol^{-1} . There is a general trend that E_A
36
37 increases with the total fraction of interstitial solutes. The same trend is visible when
38
39 each group of alloys per set of materials is considered independently (i.e. 1C versus
40
41 1.2C versus 1.6C, 17Cr-0.2C versus 17Cr-0.4C and 1.8N versus 2.2N). Unequivocally,
42
43 the experiments show that the presence of interstitial solutes increases the activation
44
45 energy for martensite formation.
46
47
48
49
50
51

52 Ferrous α martensites are classified as $\{3\ 10\ 15\}_\gamma$, $\{2\ 5\ 9\}_\gamma$, $\{2\ 2\ 5\}_\gamma$, $\{1\ 1\ 2\}_\gamma$ and $\{5$
53
54 $5\ 7\}_\gamma$ (see Refs. [18,19]). The types of martensite developing in the alloys under
55
56 investigation was determined by metallography as indicated in Table 2.
57
58
59
60
61
62

1 Table 2 reveals that the steels/alloys classified as group II develop $\{5\ 5\ 7\}_\gamma$ martensite.
2
3 Evidently, the kinetics of formation of $\{5\ 5\ 7\}_\gamma$ martensite differs from the kinetics of
4 formation of all the other types of martensite (group I): the formation of $\{5\ 5\ 7\}_\gamma$
5 martensite on cooling is suppressed by immersion in boiling nitrogen, whereas the
6 formation of all the other types of martensite is not.
7
8
9

10 In 1940 [20], Foerster and Scheil suggested that martensite formation can take place
11 according to two distinct mechanisms, *Schiebung* and *Umklapp*. The progress of
12 *Umklapp* martensite was claimed instantaneous, contrary to time-dependent growth of
13 *Schiebung* martensite units. Experimental evidence consisted in the observation of
14 sudden changes in the electrical properties of the material during the formation of
15 *Umklapp* martensite, and not during the formation of *Schiebung* martensite. Consistently,
16 in 1958 [21], Honma showed firstly that the formation of *Umklapp* martensite yields
17 acoustic emission, whereas the formation of *Schiebung* martensite does not.
18
19
20
21
22
23
24
25
26
27
28
29
30
31

32 Thereafter, in 1966 [22], Huizing and Klostermann anticipated that $\{5\ 5\ 7\}_\gamma$
33 martensite, internally slipped $\{2\ 2\ 5\}_\gamma$ martensite and the slipped part of $\{2\ 5\ 9\}_\gamma$
34 martensite are morphologically different types of martensite formed by the same
35 mechanism (i.e. *Schiebung* martensite). Consistently, Sadovskii and Romashev showed
36 in 1978 that the growth of slipped martensite on twinned martensite in the $\{2\ 5\ 9\}_\gamma$
37 system at 77 K is time-dependent [23].
38
39
40
41
42
43
44
45
46

47 To our best knowledge, it is now established for all types of martensite but $\{5\ 5\ 7\}_\gamma$
48 that transformation events can take place within a small fraction of a second, indicating
49 instantaneous growth [24-29]. Additionally, it has been shown for all types of martensite
50 but $\{5\ 5\ 7\}_\gamma$ that the transformation can occur at temperatures as low as 4 K [3,29,30].[†]
51
52
53
54
55
56

57
58 [†] It is explicitly mentioned that, within our interpretation, strain-induced martensite is classified as $\{1\ 1\ 2\}_\gamma$.
59
60
61
62
63
64
65

1 Evidently, the kinetics of transformation can be rationalized providing that the
2 formation of *Schiebung* martensite, which corresponds to $\{5\ 5\ 7\}_\gamma$ and to a slipped
3 product growing on $\{2\ 5\ 9\}_\gamma$ and $\{2\ 2\ 5\}_\gamma$, is thermally activated and thereby
4 *suppressible*, while the formation of *Umklapp* martensite is athermal and thereby
5 *insuppressible*. This is consistent with the possibility to suppress martensite formation at
6 high temperature (cf. Refs. [10-12]).
7
8
9

10 Based on the above rationalization, E_A determined in our work is the activation
11 energy for the formation of *Schiebung* martensite. Fig. 2 indicates that E_A lies in the
12 range 8–27 kJ mol⁻¹ and increases with the fraction of interstitials. It is well known that
13 small fractions of C atoms can suppress the formation of *Schiebung* martensite in Fe-Ni
14 alloys [31-33]. Additionally, it has been established that the critical cooling rate to
15 suppress the formation of $\{5\ 5\ 7\}_\gamma$ martensite in Fe decreases linearly with the logarithm
16 of the fraction of C atoms [12]. Since small differences in C (and N) content do not
17 significantly affect ΔG , as demonstrated by an invariant M_s , it is anticipated that E_A
18 obeys a similar logarithmic dependence on the fraction of interstitials (Fig. 2b).
19
20
21
22
23
24
25
26
27
28
29
30
31
32
33
34
35
36

37 In a molecular dynamics study [34], Bos et al. studied the movement of the
38 b.c.c./f.c.c. interface in Fe and obtained an effective activation energy of 6 kJ mol⁻¹ for
39 the movement of a martensite/austenite interface. Surprisingly, this value is consistent
40 with extrapolation of data in Fig. 2b to a very low content of interstitials. Borgenstam
41 and Hillert treated martensitic transformations as a common chemical reaction and
42 estimated E_A to 7 kJ mol⁻¹ for Fe-Ni-Mn and Fe-Cr-Ni alloys forming martensite
43 isothermally at cryogenic temperatures [35]. This value is also consistent with data in
44 Fig. 2b.
45
46
47
48
49
50
51
52
53
54
55
56

57 At present, there is insufficient information to conclude about the rate-controlling
58
59
60
61
62
63
64
65

1 mechanism for *Schiebung* martensite. Fascinating is the possibility that *Schiebung*
2
3 martensite is the product of a transformation that is not strictly martensitic [36]. For
4
5 martensitic transformations the austenite/martensite interface is (presumed) glissile.
6
7 Unequivocal evidence for a glissile interface is the formation of martensite at 4 K
8
9 [37,38]. To our best knowledge, martensite formation at 4 K has hitherto not been
10
11 demonstrated for $\{5\ 5\ 7\}_\gamma$ martensite. Maki and co-workers recently claimed that the
12
13 austenite/martensite interface for $\{5\ 5\ 7\}_\gamma$ and for internally slipped $\{2\ 5\ 9\}_\gamma$ is sessile
14
15 [39,40]. A sessile interface cannot move conservatively, implying that its movement is
16
17 thermally activated. In this sense, the movement of the interface could be the rate-
18
19 determining mechanism for the formation of *Schiebung* martensite and inhibit its
20
21 development at 4 K.
22
23
24
25
26
27
28
29

30 To summarize, the present investigation shows that ferrous alloys and steel can be
31
32 classified into two kinetic groups: in alloys of group I, martensite forms during
33
34 immersion in boiling nitrogen; in alloys of group II, the formation of martensite on
35
36 cooling in boiling nitrogen is suppressed. In both cases, martensite can form on re-
37
38 heating to room temperature.
39
40
41

42 There is a relationship between the transformation kinetics and the features of the
43
44 developing martensite: twinned martensite and slipped martensite formed along $\{1\ 1\ 1\}_\gamma$
45
46 shear bands (including strain-induced) correspond to kinetics group I; $\{5\ 5\ 7\}_\gamma$
47
48 martensite to kinetics group II.
49
50
51

52 All experimental observations can be rationalized considering that two distinct types
53
54 of martensite exist: *Schiebung* martensite, which is suppressible and cannot form at 4 K,
55
56 and *Umklapp* martensite, which is un-suppressible and does form at temperature
57
58
59
60
61
62
63
64
65

1 approaching absolute zero.
2

3 The activation energy for the formation of *Schiebung* martensite increases with the
4 fraction of interstitials and for the investigated alloys ranges from approx. 8 kJ mol⁻¹ to
5
6 27 kJ mol⁻¹.
7
8
9

10
11
12 This work was financially supported by the Danish Council for Independent Research
13 [grant number: DFF-4005-00223]. Eric J. Mittemeijer, Max Planck Institute for
14 intelligent systems, Stuttgart, DE, is acknowledged for fruitful discussion in an early
15 stage of this work and for supplying the Fe-C and the Fe-15Cr-13Ni alloys.
16
17
18
19
20
21
22
23
24
25

26 **References**

- 27
28
29 [1] G.V. Kurdjumov and O.P. Maksimova, Dokl Akad Nauk SSSR, 61.1 (1948), 83–86.
30
31 [2] B.S. Lement, Il Nuovo Cimento, 1.S4 (1955), 295–322.
32
33 [3] S.A. Kulin and M. Cohen. Trans. AIME, 188.9 (1950), 1139–1143.
34
35 [4] R.F. Bunshah, R.F. Mehl. Trans. AIME, 197.9 (1953), 1251–1258.
36
37 [5] M. Cohen, Trans. AIME 212.2 (1958), 171–183.
38
39 [6] N.N. Thadhani, M.A. Meyers, “Prog. Mater. Sci. 30 (1986) 1–37.
40
41 [7] A. Borgenstam, M Hillert, Acta Mater. 48:11 (2000) 2777–2785.
42
43 [8] T. Kakeshita, K. Kuroiwa, K. Shimizu, T. Ikeda, A. Yamagishi, M. Date, Mater.
44 Trans. Jim 34.5 (1993) 423–428.
45
46 [9] A.N. Holden, Acta Metall., 1.1 (1953), 617–623
47
48 [10] E.A. Wilson, ISIJ Int. 34:8 (1994) 615–630.
49
50 [11] D. A. Mirzayev, M.M. Shteynberg, T. N. Ponomareva, V.M. Schastlivtsev, Phys.
51 Met. Metallogr. 47:1 (1979) 102–111.
52
53
54
55
56
57
58
59
60
61
62
63
64
65

- 1 [12] D. A. Mirzayev, M.M. Shteynberg, T. N. Ponomareva, V.M. Schastlivtsev, Phys.
2
3 Met. Metallogr. 47:5 (1979) 73-79.
4
5 [13] M. Villa, H.F. Hansen, M.A.J. Somers, "Martensite formation in Fe-C alloys at
6
7 cryogenic temperatures", submitted for publication
8
9 [14] M. Villa, T. Christiansen, M.F. Hansen, M. AJ Somers, Metall. Ita., 11:12 (2015)
10
11 39-46.
12
13 [15] M. Villa, M.F. Hansen, K. Pantleon, M.A.J. Somers, Mater. Sci. Technol., 31:11
14
15 (2015) 1355-1361.
16
17 [16] E.J. Mittemeijer, J. Mater Sci, 27:15 (1992) 3977-3987.
18
19 [17] W. Baumann, A. Leineweber, E.J. Mittemeijer, J. Mater. Sci. 45 (2010) 6075-6082.
20
21 [18] P.G. McDougall, C.M. Wayman, The crystallography and morphology of ferrous
22
23 martensites, in: Martensite - A tribute to Morris Cohen, (Eds.) G.B. Olson, W.S.
24
25 Owen, ASM International, Cleveland, 1992, pp. 59-96
26
27 [19] T. Maki, Morphology and Substructure of Martensite in Steels, in: Phase
28
29 Transformations in Steels 2, E. Pereloma and D.V. Edmonds (Eds.), 2012, pp. 34-
30
31 58.
32
33 [20] F. Foerster, E. Scheil, Ztsch. Metallkunde 32:6 (1940) 165-173.
34
35 [21] T. Honma, DENKI-SEIKO 29:4 (1958) 261-276.
36
37 [22] R. Huizing, J.A. Klostermann, Acta Metall. 14:12 (1966) 1693-1702.
38
39 [23] V.D. Sadovskii, L. N. Romashev, Soviet Physics - Doklady 23:1 (1978) 77-79.
40
41 [24] G.R. Speich, A.J. Schwoeble, Acoustic emission during phase transformation in
42
43 steel, in: Monitoring Structural Integrity by Acoustic Emission ASTM-SPT571,
44
45 1975, pp. 40-58.
46
47
48
49
50
51
52
53
54
55
56
57
58
59
60
61
62
63
64
65

- 1 [25] Y. Sano, S.N. Chang, M.A. Meyers, S. Nemat-nasser, *Acta Metall. Mater.*, 40.2
2
3 (1992) 413-417.
4
5
6 [26] S.N. Chang, M. A. Meyers. *Acta Metall.* 36.4 (1988) 1085-1098
7
8 [27] M.A. Meyers, J. R. C. Guimaraes, *Mater. Sci. Eng.* 24.2 (1976) 289–292.
9
10 [28] K. Takashima, Y. Higo, S. Nunomura, *Philos. Mag. A* 49:2 (1984) 231–241.
11
12 [29] T. Kakehita, T. Saburi, K. Kindo, S. Endo, *Phase Trans.* 70:2 (1999) 65-113.
13
14 [30] R.P. Reed, The plate-like martensite transformation in Fe-Ni alloys, *Acta Metal.* 15
15
16 (1967) 1287-1296.
17
18
19 [31] R.B.G. Yeo, *ASM Trans. Quarterly* 57:1 (1964) 48-61.
20
21 [32] C. Crussard, J. Philibert, *Revue De Metallurgie* 53:12 (1956) 973-980.
22
23 [33] V. Raghavan, M. Cohen, *Metall. Trans.* 2:9 (1971) 2409-18.
24
25 [34] C. Bos, J. Sietsma, B.J. Thijsse, *Physical Review B* 73:10 (2006) 104117.
26
27 [35] A. Borgenstam, M. Hillert, *Acta Mater.* 45:2 (1997) 651–662.
28
29 [36] D.A. Mirzayev, M.M. Shteynberg, T. N. Ponomareva, B. Ya. Bylskiy, S. Ye
30
31 Karzunov, *Phys. Met. Metallogr.* 51:2 (1981) 116–127.
32
33 [37] F. J. Schoen, W. S. Owen, *Scripta Metall.* 5:4 (1971) 315–317.
34
35 [38] H.K.D.H. Bhadeshia, C.M. Wayman, *Phase Transformations: Nondiffusive*. In: D.
36
37 Laughlin and K. Hono (Eds.) *Physical 706 Metallurgy*, 5th edn, vol I, Ch. 9, 1021-
38
39 1072 (Elsevier, 2014).
40
41
42
43
44
45
46 [39] A. Shibata, T. Furuhashi, T. Maki, *Acta Mater.* 58 (2010) 3477–3492.
47
48
49 [40] T. Moritami, N. Miyajima, T. Furuhashi, T. Maki, *Scripta Mater.* 47 (2002) 193–199.
50
51
52
53
54
55
56
57
58
59
60
61
62
63
64
65

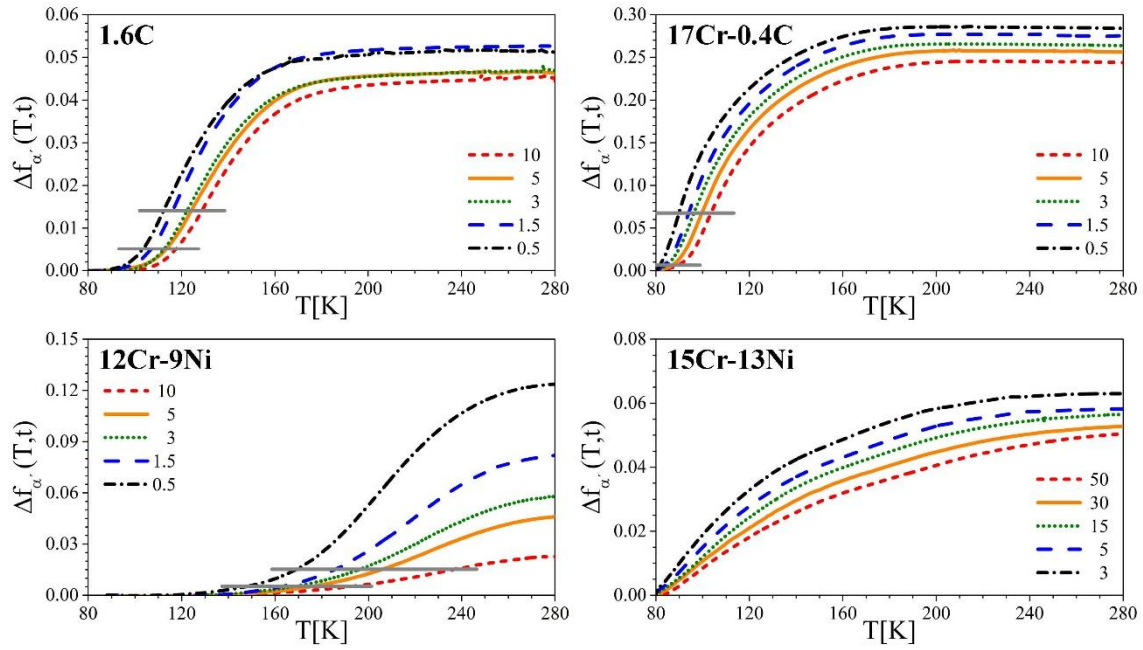


Fig.1 Examples of martensite formation during isochronal heating from 80 K: fraction of martensite, Δf , plotted versus temperature, T . Numbers in the legend refer to the heating rate applied, ϕ , expressed in K min^{-1} . The grey horizontal lines indicate the intervals used to calculate E_A . Data for 1.6C and 17Cr-0.4C are chosen as representative for the Fe-C alloys and the Fe-Cr-C steels, respectively. Data referring to the Fe-N alloys, to 100Cr6 and to the PH steels were presented earlier [14].

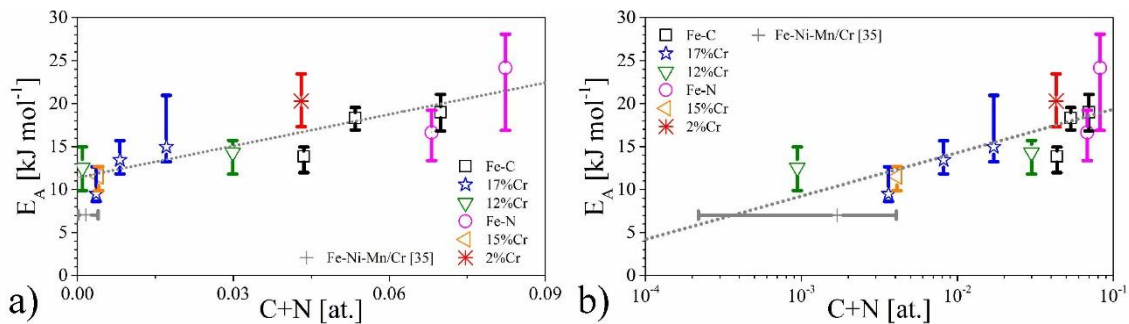


Fig.2 Activation energy for thermally activated martensite formation E_A plotted versus the atomic fraction of interstitial solutes in the material, $C+N$, expressed in (a) linear scale and (b) logarithmic scale.

Figure 1
[Click here to download high resolution image](#)

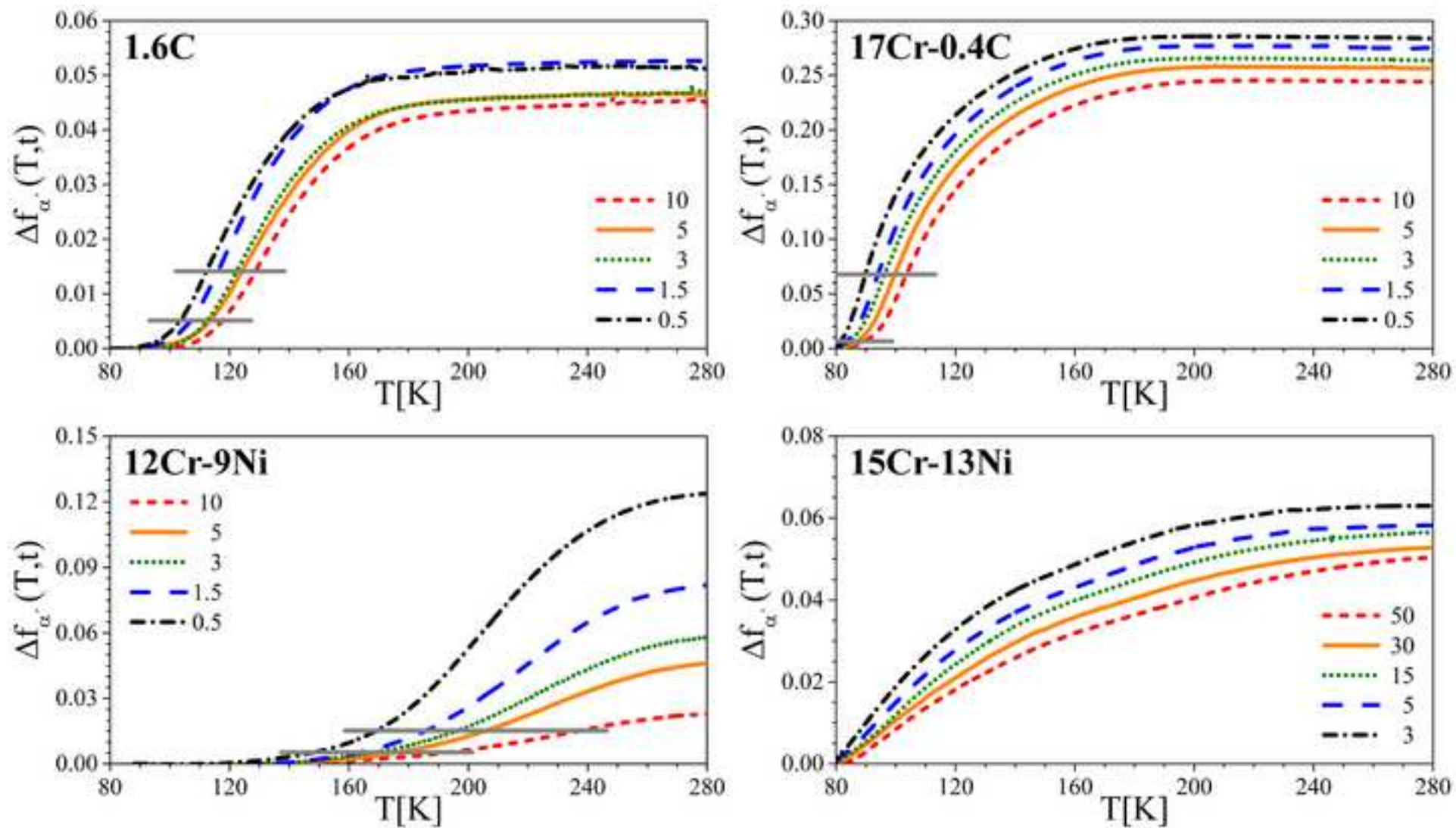


Figure 2
[Click here to download high resolution image](#)

